

## Article

# Antimicrobial and Photocatalytic Activities of Selenium Nanoparticles Synthesized from *Elaeagnus indica* Leaf Extract

Dhatchanamoorthi Indhira <sup>1,†</sup>, Arumugam Aruna <sup>2,†</sup>, Krishnamoorthy Manikandan <sup>1,3</sup>, Mohammed F. Albeshr <sup>4</sup>, Abdulwahed Fahad Alrefaei <sup>4</sup>, Ramachandran Vinayagam <sup>5,†</sup>, Arumugam Kathirvel <sup>6</sup>, Selvaraj Ranjith Priyan <sup>7</sup>, Govindan Suresh Kumar <sup>7,\*</sup> and Ramalingam Srinivasan <sup>8,\*</sup>

<sup>1</sup> Department of Biotechnology, K. S. Rangasamy College of Arts and Science (Autonomous), Tiruchengode 637 215, Tamil Nadu, India

<sup>2</sup> Department of Biotechnology, Sri Kailash Women's College, Thalavaiasal, Attur 636 112, Tamil Nadu, India

<sup>3</sup> Department of Science, School of Health & Life Science, Teesside University, Tees Valley, Middlesbrough TS1 3BX, UK

<sup>4</sup> Department of Zoology, College of Sciences, King Saud University, P.O. Box 2455, Riyadh 11451, Saudi Arabia

<sup>5</sup> Department of Biotechnology, Institute of Biotechnology, Life and Applied Sciences, Yeungnam University, Gyeongsan-si 38541, Gyeongsangbuk-do, Republic of Korea

<sup>6</sup> Department of Chemistry, K. S. Rangasamy College of Arts and Science (Autonomous), Tiruchengode 637 215, Tamil Nadu, India

<sup>7</sup> Department of Physics, K. S. Rangasamy College of Arts and Science (Autonomous), Tiruchengode 637 215, Tamil Nadu, India

<sup>8</sup> Department of Horticulture & Life Science, Yeungnam University, Gyeongsan-si 38541, Gyeongsangbuk-do, Republic of Korea

\* Correspondence: gsureshkumar1986@gmail.com (G.S.K.); sribt27@gmail.com (R.S.)

† These authors contributed equally to this work.



**Citation:** Indhira, D.; Aruna, A.; Manikandan, K.; Albeshr, M.F.; Alrefaei, A.F.; Vinayagam, R.; Kathirvel, A.; Priyan, S.R.; Kumar, G.S.; Srinivasan, R. Antimicrobial and Photocatalytic Activities of Selenium Nanoparticles Synthesized from *Elaeagnus indica* Leaf Extract. *Processes* **2023**, *11*, 1107. <https://doi.org/10.3390/pr11041107>

Academic Editors: Adriana Trifan, Izabela Korona-Główniak and Ibrahim M. Abu-Reidah

Received: 23 February 2023

Revised: 25 March 2023

Accepted: 2 April 2023

Published: 4 April 2023



**Copyright:** © 2023 by the authors. Licensee MDPI, Basel, Switzerland. This article is an open access article distributed under the terms and conditions of the Creative Commons Attribution (CC BY) license (<https://creativecommons.org/licenses/by/4.0/>).

**Abstract:** Selenium nanoparticles (Se NPs) have recently received much interest due to their low toxicity, high bioavailability, and wide applications. This study synthesized Se NPs using selenious acid as a starting material and leaf extract from *Elaeagnus indica* as a reducing agent. Spectroscopic and electron microscopy investigations have demonstrated the production of aggregated amorphous Se NPs with phytochemicals. Furthermore, the reduction of selenious acid into Se NPs by phytochemicals present in the leaf extract of *E. indica* was confirmed in a prominent band at 269 nm in the UV-visible spectrum. The biosynthesized selenium nanoparticles have a 10–15 nm particle size distribution. The agar well diffusion assay exhibited remarkable dose-dependent, wide-spectrum antimicrobial efficacy of the Se NPs against all the tested microorganisms. Moreover, the lowest minimum inhibitory concentration (10 µg/mL) was noted against *Salmonella* Typhimurium and *Fusarium oxysporum*. The prepared Se NPs degraded methylene blue dye by about 89% after 6 h of exposure to sunlight. In conclusion, the synthesis of Se NPs using *E. indica* leaf extract shows promise as a method for producing Se NPs with significant antimicrobial activity and potential for methylene blue photodegradation. These properties make them potentially valuable in various fields, including water treatment and biomedical applications, in the future.

**Keywords:** green synthesis; Se NPs; *Elaeagnus indica*; photocatalytic activity; antimicrobials

## 1. Introduction

Nanotechnology is becoming a tremendously attractive area of study in material science; it entails the manipulation of matter on the nanoscale via the application of innovative physical and chemical processes to produce new materials with unique features. In recent years, this field has seen substantial development [1,2]. Nanoparticles have a variety of distinct advantages, such as a larger surface area to volume ratio and quantum confinement, resulting in enhanced performance in a range of applications. Several of

these benefits of nanomaterials have been employed in the management of energy, the control of environmental contamination, and the treatment of health issues because of their novel properties that their bulk materials cannot deliver [3,4]. Nowadays, the rise in antibiotic-resistant bacteria has led researchers to focus on the development of novel nanomaterial-based antimicrobial agents over synthetic antibiotics [5,6].

Similarly, industrialization and urbanization have caused a critical problem of environmental pollution worldwide. Mainly aquatic pollution caused by industrial waste harms both aquatic and terrestrial life, leading to significant economic losses [7]. Furthermore, organic dyes are harmful to the environment and non-biodegradable, leading to deadly diseases such as human cancer. Although various modern technologies, such as adsorption, filtration, reduction, precipitation, electrolysis, flocculation, coagulation, and microbially mediated process, are available to combat water pollution, they come with certain limitations, such as high costs and the use of harmful chemicals [3,7]. Hence, an urgent need to clean up this polluted water has led to the developing of advanced new technologies [8]. Recently, photocatalytic nanomaterials have gained significant attention due to their potential to mitigate contamination in aquatic environments through photocatalytic processes [9]. Hence, developing nanomaterials for various applications has attracted significant interest recently. Many different types of nanomaterials have been developed and used in various aspects [10,11].

Selenium (Se) is a nonmetal that exists in three forms: amorphous Se, crystalline trigonal, and crystalline monoclinic. Selenium is a significant material that can be used to mitigate environmental pollution and act as an antimicrobial agent [12]. Moreover, selenium is a trace element required for living organisms and is crucial in various critical biological processes. Due to its unique chemical, physical, and biological characteristics, selenium has garnered significant interest in photocatalysis, biosensing, antimicrobial applications, diagnostics, and therapy [13]. Nanomaterials can be synthesized using various bottom-up approaches, such as sol-gel, precipitation, hydrothermal, microemulsion, sonochemical, and microwave-assisted processes [14–16]. However, most bottom-up techniques have some drawbacks, such as hazardous chemicals, complex methodology, limited product efficiency, and significant energy consumption [4,17]. Similarly, the chemical and physical nanoparticle synthesis techniques have resulted in hazardous effluents or expensive processes [18,19]. Owing to the drawbacks of chemical and physical NPs, synthesis techniques lead to the finding of novel methods which rectify these problems. Moreover, the cellular uptake of inorganic Se NPs is lower than the organic form, limiting their biological applications. Therefore, synthesizing Se NPs using biomolecules can enhance their biocompatibility and stability. One such alternative method is the green synthesis of selenium nanoparticles (Se NPs), which has gained considerable attention due to its numerous advantages [20].

Different plant, fungal, and bacterial species and their extracts have been used as reducing agents in the process of NPs synthesis [21,22]. Biomolecules generally act as reducing agents that convert  $\text{Se}^{4+}$  (selenate) or  $\text{Se}^{6+}$  (selenite) to  $\text{Se}^0$  to produce Se NPs [23]. Therefore, plant extracts have been used as both reducing and stabilizing agents in the green synthesis of Se NPs, which have been extensively investigated for their potential applications in photocatalysis and antimicrobial activity [20,23]. Further, previous studies have indicated that the concentration and reduction potential of the phytochemicals present in the plant extracts directly influence the phytofabrication of Se NPs [15–22,24–28]. In addition, several secondary metabolites from plants are reported to exhibit various biological functions [29]. Therefore, the presence of phytochemicals in nanoparticles can provide additional functional properties to the nanoparticles [30]. Consequently, various plants are being explored to synthesize selenium nanoparticles for various environmental and biomedical applications.

*Elaeagnus indica* Servett, a member of the *Elaeagnaceae* family, is found in the Eastern Ghats region of India [31]. *E. indica* contains various phytochemicals, including polyphenolics, flavonoids, tannins, alkaloids, fixed oils, glycosides, saponins, steroids, and proteins.

Furthermore, extracts of *E. indica* exhibit significant antioxidant larvicidal, antimicrobial, antiproliferative, and anti-inflammatory activities [32,33]. Previous studies have indicated that silver, copper, and zinc-based nanoparticles synthesized using *E. indica* extracts exhibit significant antimicrobial and light-dependent organic dye degradation potential [7,34]. However, there is limited research on using *E. indica* extract for nanoparticle production. To our knowledge, no reports on synthesizing selenium nanoparticles using *E. indica* extract exist. Therefore, this study aims to fill this research gap using a simple and environmentally friendly approach for synthesizing selenium nanoparticles using *E. indica* leaf extract. Additionally, we investigated the antimicrobial potential and photocatalytic degradation ability of biosynthesized Se NPs nanoparticles against methylene blue dye.

## 2. Materials and Methods

### 2.1. Chemicals

Ciprofloxacin, dimethyl sulfoxide (DMSO), fluconazole, *p*-iodonitrotetrazolium, methylene blue (MB), Müller Hinton broth, Müller Hinton agar, Sabouraud dextrose broth, Sabouraud dextrose agar, and selenous acid were purchased from Himedia Laboratories, Mumbai, India. All the reagents/chemicals used in this study were analytical grade and used as supplied. All the experiments were performed with double-distilled water.

### 2.2. Plant Source and Extraction

The fresh, young, and healthy leaves of *Elaeagnus indica* were collected from the Kollu Hills (latitude—11.316098 and longitude—78.349249) in the Namakkal district of Tamil Nadu, India. The taxonomy of the collected plant material (Reference letter No: BSI/SRC/5/23/2014-15/Tech/1942) was confirmed by the Botanical Survey of India (BSI) in Coimbatore, Tamil Nadu, India. The collected plant materials were washed with running tap water followed by double-distilled water to remove any solid dust particles; later, leaves were dried for two weeks at room temperature in dark. Dried leaves were pulverized, sieved using a 100 mesh sifter, and stored in an air-tight bag. These powdered components were used for phytochemical extraction. A 50 g *E. indica* leaf powder was loaded in a Soxhlet apparatus and double-distilled water was used as extractive solvent. The plant material was extracted until the efflux solvent was colorless. Further, the extract was filtered using Whatman filter paper (No. 1) and kept at 4 °C in a sealed container until it was utilized for the synthesis of nanoparticles.

### 2.3. Synthesis of Se NPs

The synthesis of selenium nanoparticles was carried out by the method [35] with some modifications. Selenous acid is used as the starting material for synthesizing Se NPs. The prepared *E. Indica* extract solution (200 mL) was mixed with 50 mM of selenous acid while vigorously being stirred in a conical flask. The mixture was agitated continuously for 24 h at room temperature. Next, the reaction mixture was centrifuged for 20 min at 4000 rpm to remove unreacted reactants. The nano pellets were washed with distilled water, then acetone, and centrifuged. Then, the obtained precipitates were subjected to drying at 110 °C and ground into powder for further analysis.

### 2.4. Characterization of Synthesized Se NPs

#### 2.4.1. X-ray Diffraction Analysis

The XRD pattern of the synthesized Se NPs was recorded with a step size of 2°/min in a X'Pert Pro X-ray diffractometer (PANalytical, Malvern, UK) with current settings of 30 mA and voltage settings of 40 kV in the 2 $\theta$  range of 10–80° using CuK $\alpha$  X-ray source ( $\lambda = 1.5406 \text{ \AA}$ ).

#### 2.4.2. Fourier Transform Infrared Spectroscopy (FTIR) Analysis

For FTIR analysis, 100 mg of KBr powder with 2 mg of the prepared specimen was mixed to form thin discs using a pelletizer. The prepared disc sample was examined in

the range of 400 to 4000  $\text{cm}^{-1}$  by a Perkin Elmer RX-I (Perkin Elmer, Waltham, MA, USA), FT-IR spectrometer with a resolution of 1  $\text{cm}^{-1}$ .

#### 2.4.3. Particle Size Analyzer

The particle size distribution of the synthesized specimen was examined using a particle size analyzer (NANOPHOX, Sympatec GmbH, Clausthal, Germany). A disposable acrylic glass cuvette was used for measurement. Automated cuvette placement and accurate laser intensity control to optimize measuring signal facilitates quick measuring.

#### 2.4.4. Scanning Electron Microscopy (SEM) and EDX

SEM (JSM-6360, JEOL, Japan) at voltage 7.50 kV was used to conduct a morphological examination on a sample obtained by vacuum drying a drop of NPs solution on a graphite grid. The elements present in the prepared specimen were micro-analyzed on the SEM by an energy-dispersive X-ray microanalyzer (EDS, Oxford INCA, Abingdon, Oxfordshire, UK).

#### 2.4.5. Transmission Electron Microscopy (TEM)

TEM (model JEM 2100, JEOL, Tokyo, Japan), was used to analyze the particle size and shape. Acetone was used to disperse the powdered material on a carbon-coated copper grid before it was allowed to dry so that TEM imaging could be performed.

### 2.5. Antimicrobial Activity

#### 2.5.1. Agar Well Diffusion Assay

The antimicrobial activity of the synthesized Se NPs was evaluated against four clinically isolated bacteria (two Gram-positive bacteria (*Bacillus subtilis* and *Staphylococcus epidermidis*) and two Gram-negative bacteria (*Salmonella* Typhimurium and *Klebsiella pneumoniae*) as well as two clinically isolated fungal pathogens (*Fusarium oxysporum* and *Aspergillus niger*) by agar well diffusion method as previously described [7]. A total of 5 mL of Müller Hinton broth (MHB) was used to grow the mother culture of selected bacterial strains in a shaking condition (for 16 h) at 37 °C to obtain a turbidity of  $1.5 \times 10^8$  CFU. Similarly, 5 mL of Sabouraud dextrose broth (SDB) was inoculated with fungal cultures and incubated at room temperature for 72 h to obtain an effective fungal mass of  $1 \times 10^6$  CFU for antifungal activity. Agar well diffusion test was performed using 10 mg of the prepared nanoparticles dispersed in 1 mL of DMSO. A 50  $\mu\text{L}$  suspension of the selected bacterial and fungal cultures was swabbed on the Müller Hinton agar (MHA) and Sabouraud dextrose agar (SDA) plates, respectively, using a sterilized cotton swab. After swabbing, a 5 mm sterile cork borer was used to bore five holes at equal distances on each MHA and SDA medium plate. Then, 50  $\mu\text{L}$  of the prepared Se NPs suspension at various concentrations (25, 50, and 75  $\mu\text{g}$ ) was loaded into wells and diffused at room temperature. Fluconazole (1  $\mu\text{g}/\text{mL}$ ) and ciprofloxacin (1  $\mu\text{g}/\text{mL}$ ) were used as positive controls for fungi and bacteria, respectively, and an equal amount of DMSO was used as a negative control. The bacterial and fungal plates were incubated at 37 °C for 24 h and 72 h at room temperature, respectively. After the incubation period, the diameter of the growth inhibition zone was measured and recorded.

#### 2.5.2. Minimum Inhibitory Concentration (MIC)

The broth micro-dilution bioassay method was used to measure the MIC values of synthesized Se NPs. This test was carried out according to the method of Srinivasan et al. (2017). Briefly, 100  $\mu\text{L}$  of different concentrations (1, 5, 10, 15, 20, 25, 30, 40, 50, and 75  $\mu\text{g}/\text{mL}$ ) of Se NPs was mixed with an equal volume of medium (MHB for bacteria and SDB for fungus) into 96 well microplates. A 20  $\mu\text{L}$  microbial culture was introduced to each well, and the microplate was incubated in appropriate growth conditions, as mentioned in Section 2.5.1. After incubation, 40  $\mu\text{L}$  of *p*-iodonitrotetrazolium (0.2 mg/mL, as a growth indicator) was introduced to each well and again incubated for 1 h. The development of

red color indicated the microbial growth in wells. The lowest concentration of the Se NPs in which red color development was not found was recorded as MIC value.

### 2.6. Photocatalytic Activity

A 10 mg of prepared Se NPs was added to 100 mL (50 mg/L) of aqueous MB solution and magnetically agitated for 30 min to reach equilibrium. Then, it was subjected to sunlight and the photocatalytic activity of Se NPs was recorded between sunrise and sunset. At appropriate time intervals, aliquots of 2–3 mL supernatant were filtered to test the photodegradation of MB dye. The absorption spectra of the supernatant were observed using a UV-Vis spectrophotometer (Hitachi, Japan). The quantity of dye undergoing disintegration was determined from the standard calibration based on the highest absorbance at 660 nm [7,36]. Furthermore, an experiment serving as a control was conducted without sunlight and Se Nps.

## 3. Results and Discussion

### 3.1. Characterization of Synthesized Se NPs

X-ray diffraction (XRD) was performed to investigate the crystalline behavior of the synthesized Se Nps. Figure 1a shows the XRD pattern of the prepared Se NPs specimen. It exhibited a broad peak at roughly  $2\theta = 19\text{--}25^\circ$  without any sharp Bragg reflections, indicating the amorphous nature of Se NPs [24]. Previous studies have shown that plant extracts can produce amorphous Se NPs [25,26], which coincides with the present study's findings. By contrast, crystalline selenium has a crystal structure with prominent and sharp peaks at  $2\theta = 24^\circ$  and  $30^\circ$  [27]. It is necessary to heat the as-prepared Se NPs around  $400^\circ\text{C}$  to attain crystalline form. However, it may eliminate bioactive molecules essential to this green product's antibacterial function. Hence, we have intentionally used as-prepared Se NPs for further studies. The FTIR spectrum of Se NPs is shown in Figure 1b, which was acquired in the mid-IR range between  $400$  and  $4000\text{ cm}^{-1}$ . The bands identified at  $3272\text{ cm}^{-1}$ ,  $2915\text{ cm}^{-1}$ ,  $1640\text{ cm}^{-1}$ ,  $1330\text{ cm}^{-1}$ , and  $1059\text{ cm}^{-1}$  correspond to O–H, C–H, C = O, C = C, and N–H bonds, respectively, which correlated with the functional groups of phytochemicals such as alcohols, alkenes, amines, flavonoids, and carboxylic acids [37,38]. The bands detected at  $540\text{ cm}^{-1}$  related to the stretching vibration of the C–S bond in the organic residue [31]. Based on these results, it is possible to assert that the biomolecules derived from leaf extract were responsible for capping the surface of the Se NPs and that they play a significant role in the synthesis of Se NPs.

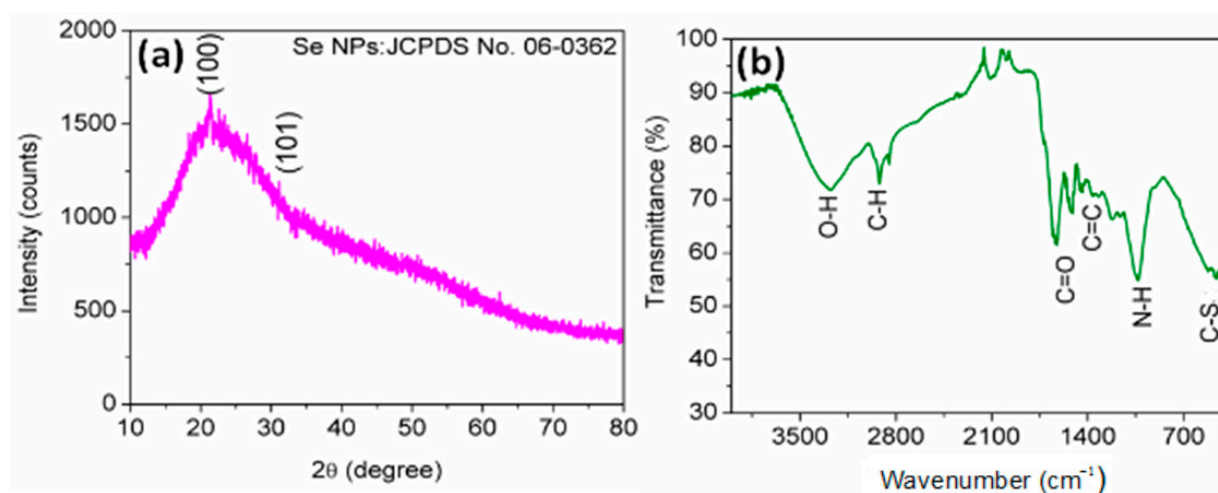


**Figure 1.** (a) XRD pattern and (b) FTIR spectrum of synthesized Se NPs.

The formation of Se NPs from plant extract was confirmed by the results of UV-visible spectroscopy analysis (Figure 2a). In general, 200–800 nm wavelengths of light were used to characterize the formation of metal oxide nanoparticles. The chemically reduced Se

NPs were detected in a prominent band at 269 nm, corresponding to the surface plasmon resonance of the Se NPs; this indicated that the synthesis of Se NPs from plant extract was successful. This peak provided conclusive evidence for Se NPs, which was in line with the findings of the previous publications [38–40]. One of the most common approaches to determining the size of NPs is called dynamic light scattering (DLS), also known as photon correlation spectroscopy. When the Se NPs suspension is subjected to a light beam, its direction and intensity are changed due to the scattering phenomenon of Se NPs. Figure 2b depicts the particle size distribution of the synthesized Se NPs, demonstrating that the particle size distribution is in the nanoscale range. The average particle size distribution of the biosynthesized Se NPs was found to be 14 nm. The DLS analysis findings coincide with the Se NPs synthesized using *Diospyros montana* leaf extract [38].

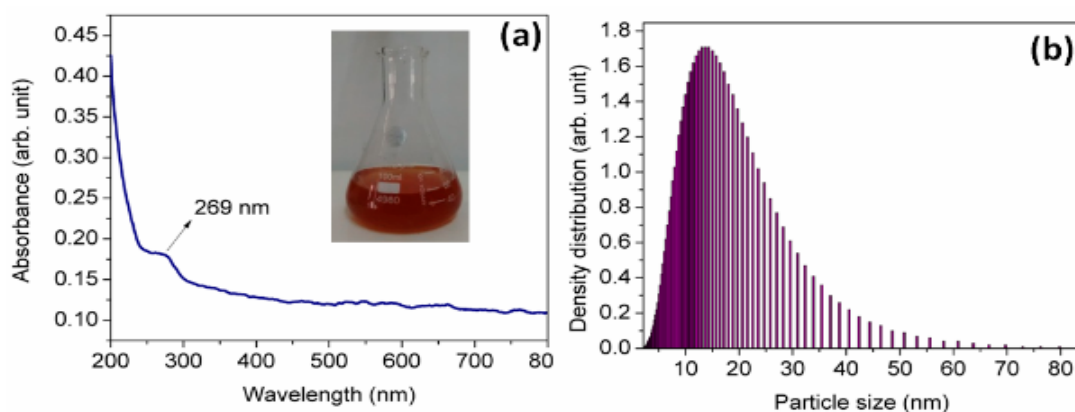


**Figure 2.** (a) UV-visible spectrum and (b) Se NPs particle size.

SEM was used to investigate the surface morphology and microscopic structure of produced Se NPs. Figure 3a shows SEM images of Se NPs obtained using an aqueous leaf extract of *E. indica* as a reducing agent. The SEM picture reveals spherical selenium nanostructures that are highly aggregated and consistently organized throughout the surface area. Agglomerated nanoparticles may be produced by nucleating and developing particles on the nanoscale scale, followed by interactions with the physical environment [41]. However, because of their tiny sizes and tendency to aggregate, the shape and size of individual particles could not be assessed with a high degree of accuracy. The results of EDX analysis revealed that the synthesized Se NPs harbor a significant amount of Se (49.88 wt.%) and O (46.16 wt.%), and a low amount (3.96 wt.%) of carbon (Figure 3b). The occurrences of carbon and oxygen in the EDX spectrum of the Se NPs were due to the presence of phytochemicals. In most cases, phytochemicals were found to be present in the Se NPs, which are synthesized using plant extracts [35,38,39]. These phytochemicals may play an essential role in the biological activities of the Se NPs [38].

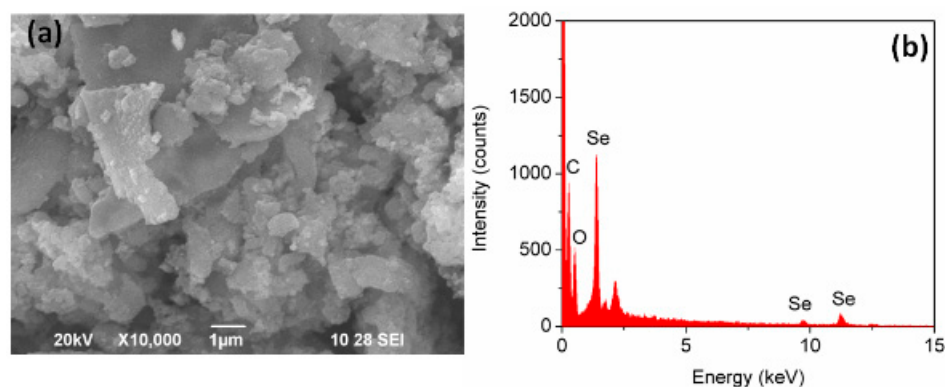


**Figure 3.** (a) SEM images and (b) EDX spectrum of synthesized Se NPs.

Figure 4 shows TEM images of synthesized Se NPs, which show spherical morphology. Nanoparticles were found to be 10–15 nm in size and homogeneous and highly agglomerated, which aligns with the SEM and DLS analysis. Polyphenols, flavonoids, and terpenoids are some of the phytochemicals found in *E. indica* leaf extract. This extract is a natural and sustainable source of reducing agents that is cost-effective and ecologically friendly. Phytochemicals found in *E. indica* leaf extract can interact with selenium precursor and control particle growth in three dimensions, leading to a spherical shape. Most publications have revealed that most green synthesis-produced Se nanoparticles are spherical [42], which agree well with the present study. Compared to the results of other published articles [28,43], the size of the Se NPs found in this study is smaller (5–10 nm).

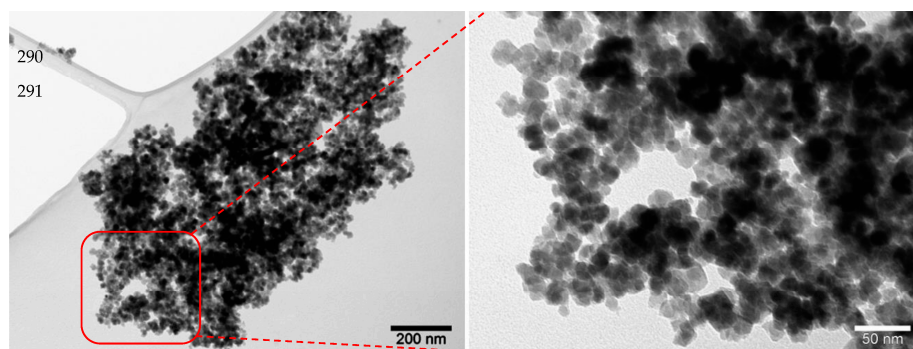


**Figure 4.** TEM images of synthesized Se NPs.

### 3.2. Antimicrobial Activity

The synthesized Se NPs showed a dose-dependent, broad-spectrum antimicrobial activity (Figure 5). The antimicrobial results revealed that the Se NPs significantly inhibited the growth of both gram-positive and gram-negative bacteria (Table 1). The high concentration (75  $\mu\text{g}$ ) of Se NPs exhibited the maximum zone of growth inhibition of  $17.67 \pm 0.47$ ,  $16.33 \pm 1.25$ ,  $18.67 \pm 0.94$ ,  $15.00 \pm 0.82$ ,  $21.33 \pm 0.47$ , and  $10.00 \pm 1.41$  mm against *B. subtilis*, *S. epidermidis*, *S. Typhimurium*, *K. pneumoniae*, *F. oxysporum*, and *A. niger*, respectively (Table 1). It should be noted that even at a low concentration of Se NPs (25  $\mu\text{g}$ ), a zone of growth inhibition of  $11.67 \pm 1.25$ ,  $9.00 \pm 0.82$ ,  $14.33 \pm 1.25$ ,  $10.33 \pm 1.25$ ,  $13.67 \pm 0.47$ , and  $7.00 \pm 0.82$  mm were found against *B. subtilis*, *S. epidermidis*, *S. Typhimurium*, *K. pneumoniae*, *F. oxysporum*, and *A. niger*, respectively. However, minimal growth inhibition was observed in the *A. niger* even at a high concentration (75  $\mu\text{g}$ ) of Se NPs tested.

**Table 1.** Antimicrobial activity of green synthesized Se nanoparticles by well diffusion method.

Organisms Name	Diameter of Zone of Inhibition (in mm)				
	25 $\mu\text{g}$ <sup>†</sup>	50 $\mu\text{g}$	75 $\mu\text{g}$	PC <sup>*</sup>	NC <sup>#</sup>
Bacteria					
<i>Bacillus subtilis</i>	$11.67 \pm 1.25$	$14.00 \pm 1.63$	$17.67 \pm 0.47$	$31.67 \pm 1.25$	$0.00 \pm 0.00$
<i>Staphylococcus epidermidis</i>	$09.00 \pm 0.82$	$15.33 \pm 0.47$	$16.33 \pm 1.25$	$31.00 \pm 0.82$	$0.00 \pm 0.00$
<i>Salmonella Typhimurium</i>	$14.33 \pm 1.25$	$17.00 \pm 0.82$	$18.67 \pm 0.94$	$34.67 \pm 0.94$	$0.00 \pm 0.00$
<i>Klebsiella pneumonia</i>	$10.33 \pm 1.25$	$14.67 \pm 0.94$	$15.00 \pm 0.82$	$30.67 \pm 0.47$	$0.00 \pm 0.00$
Fungus					
<i>Fusarium oxysporum</i>	$13.67 \pm 0.47$	$20.00 \pm 1.41$	$21.33 \pm 0.47$	$22.33 \pm 1.25$	$0.00 \pm 0.00$
<i>Aspergillus niger</i>	$07.00 \pm 0.82$	$9.33 \pm 0.47$	$10.00 \pm 1.41$	$17.00 \pm 1.63$	$0.00 \pm 0.00$

<sup>†</sup>—Amount of synthesized Se NPs. <sup>\*</sup>—Positive control (PC) for antibacterial (Ciprofloxain (1  $\mu\text{g}/\mu\text{L}$ ) and antifungal (fluconazole, 1  $\mu\text{g}/\mu\text{L}$ ) activity; <sup>#</sup>—Negative control (NC) (DMSO).

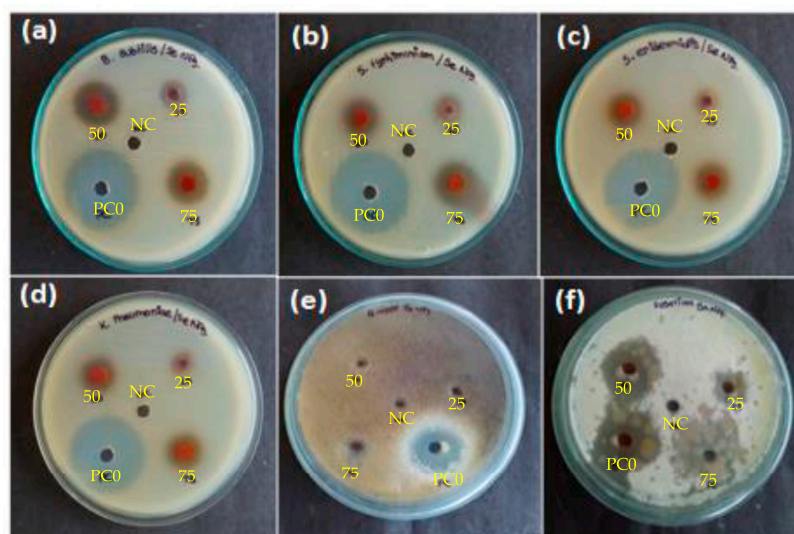


**Figure 5.** Antimicrobial activity of green synthesized Se Nps by well diffusion method (a) *Bacillus subtilis*, (b) *Salmonella Typhimurium*, (c) *Staphylococcus epidermidis*, (d) *Klebsiella pneumoniae*, (e) *Aspergillus niger*, and (f) *Fusarium oxysporum*. 25, 50, and 75 in the image were indicating the concentrations (in  $\mu\text{g}$ ) of Se Nps. PC-positive control: Fluconazole (1  $\mu\text{g}/\text{mL}$ ) and ciprofloxacin (1  $\mu\text{g}/\text{mL}$ ) for fungus and bacteria, respectively. NC-negative control (DMSO).

The MIC values of Se NPs against all the tested microorganisms were in the range of 10–25  $\mu\text{g}/\text{mL}$  except *A. niger* (Figure 6). The lowest MIC values (10  $\mu\text{g}/\text{mL}$ ) was detected in *S. Typhimurium* and *F. oxysporum*, which indicated that these microbes are more sensitive to the synthesized Se NPs. The least growth inhibition effect of Se NPs was observed in *A. niger* due to the high MIC value (75  $\mu\text{g}/\text{mL}$ ). The MIC values are correlated with the agar diffusion test. The presence of phytochemicals such as flavonoids, terpenoids, alkaloids, and other bioactive compounds in the NPs is a possible reason for the antimicrobial potential of those NPs synthesized from plant extracts [7]. These phytochemicals can inhibit the enzymes responsible for DNA replication and other gene expansion essential for the survival of microbes. Further, these compounds alternate the cell wall and or cell membrane permeability, leading to microbial cell death [7,37,44]. It is also possible that selenium nanoparticles have an antibacterial effect owing to the production of reactive oxygen species or the inactivation of enzymes, which might result in the death of microbial cells [37,44].

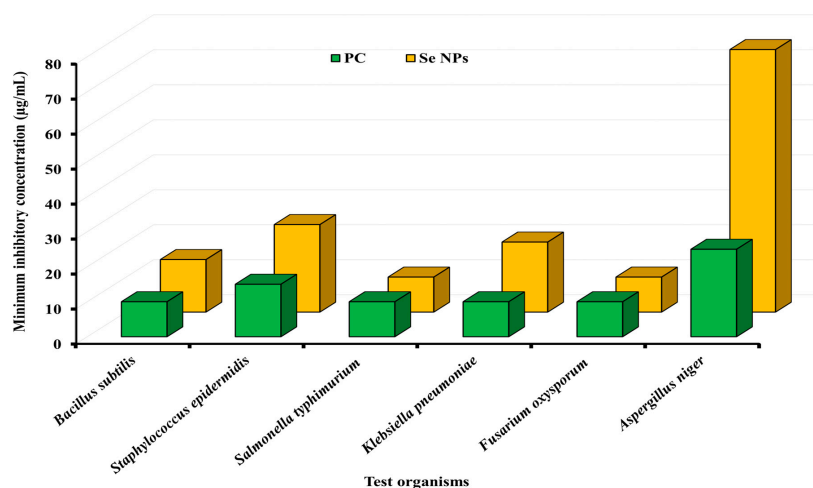


**Figure 6.** The minimum inhibitory concentration of Se NPs against various microbes. PC-positive control: fluconazole and ciprofloxacin for fungus and bacteria, respectively.

### 3.3. Photodegradation Activity

The Se NPs exhibited a significant light-dependent MB dye degradation potential (Figure 7). About 11% of MB dye degradation efficacy was noted in the dark. In contrast, the sunlight exposure increased the MB dye degradation efficiency of Se NPs up to 89% during the 6 h photoperiod. Electrons can move from the valence band to the conduction band of prepared Se NPs when the energy of solar radiation is greater than the bandgap energy. Those photogenerated electrons produced radicals such as superoxide anion radicals and OH radicals in an aqueous medium. These radicals work fast to convert the MB dye into other by-products that are not harmful [45,46]. The following reaction could take place during the process of MB being broken down by selenium nanoparticles in the presence of light.

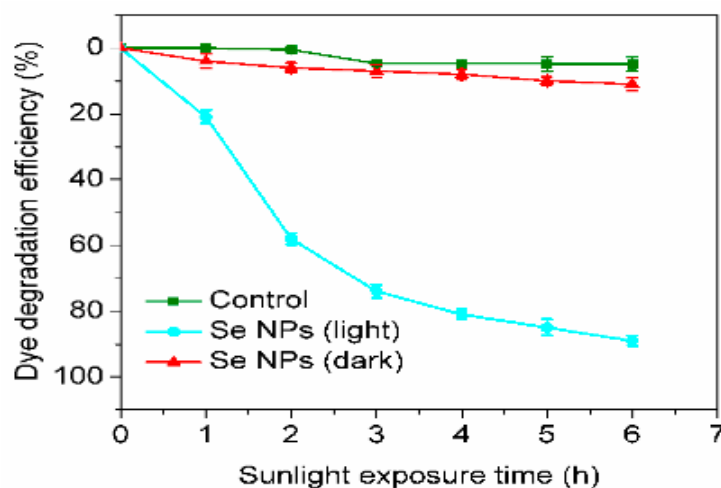
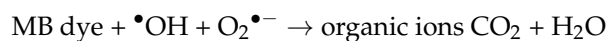
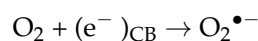
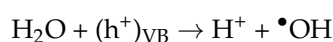
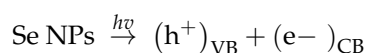


**Figure 7.** The photocatalytic degradation of MB dye by prepared Se NPs with and without sunlight irradiation.

Figure 8 illustrates the process when the prepared Se NPs are subjected to solar radiation, forming superoxide anion radicals and OH radicals. This is the consequence of the inherent characteristics and phytochemical makeup of Se NPs obtained via plant extract-mediated synthesis. This might cause fluctuations in the electronic structure, resulting in a typical photocatalytic activity [7]. Previous reports by other researchers well support this finding. Hassanien et al. studied the mechanism of the photocatalytic degradation process of Se NPs obtained using *M. Oleifera* leaves extract and found that it involved the generation of reactive oxygen species and the breaking of the azo bond in the Sunset yellow azo dye molecule [47]. Moreover, Menon et al. showed that the biosynthesized selenium nanoparticles were highly effective in the degradation of the three industrial dyes (Methylene Orange dye, Coomassie Brilliant Blue, Bromophenol Blue) with high degradation efficiencies [48].

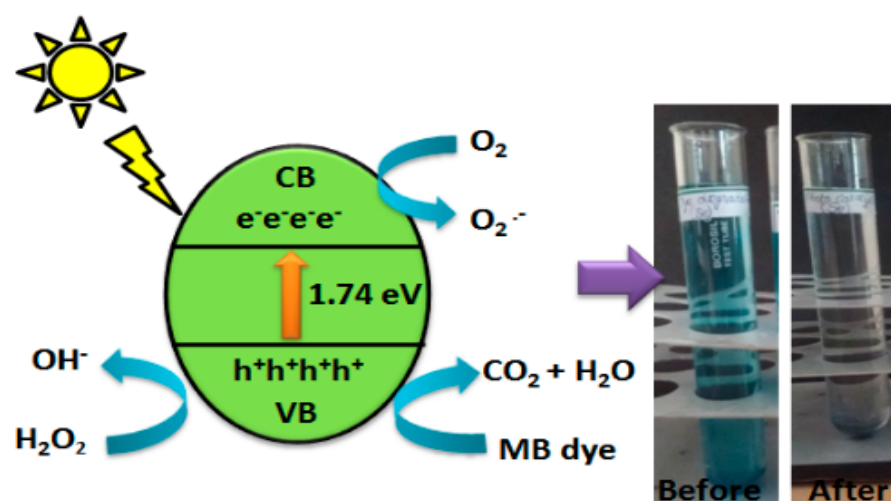


**Figure 8.** Schematic representation of the photodegradation of MB dye by the prepared Se NPs under sunlight irradiation.

The present study is the first report on synthesizing Se NPs using *E. indica* leaf extract. Chemical synthesis is the most prevalent method used to manufacture Se NPs. However, this method often involves using hazardous chemicals such as sodium borohydride, which, when combined with water, may produce explosive or combustible gases. The production of Se NPs via biosynthesis from plant extracts is less harmful to the environment since it does not result in the formation of any hazardous chemicals [28,49]. Moreover, selenium is vital for human health, with a daily need of 300  $\mu\text{g}$  [50]. Selenium is an essential trace element in most organisms and plays a crucial role in the scavenging of free radicals, the prevention of oxidation, and the retardation of the aging process in living systems [50,51]. The absorption of Se NPs from antibacterial products such as ointments or gels may not be hazardous since selenium plays a function in the body's homeostasis. Se NPs outperform other products such as silver or gold nanoparticles [28]. The prepared Se NPs in this study act as a potential antimicrobial for a wide range of microorganisms and as a better photocatalyst for the degradation of MB dye.

#### 4. Conclusions

The present study successfully produced Se NPs using selenous acid as the raw material and *E. indica* leaves extract as a reducing agent. The results of spectral and microscopy studies such as XRD, FTIR, DLS, UV-visible, SEM, TEM, and EDX conclude that the formation of aggregated amorphous Se NPs were associated with the phytochemicals from *E. indica* extract. The outcome of the DLS analysis indicated that the particle size distribution of the biosynthesized selenium nanoparticles was averaged to be 14 nm. The synthesized Se NPs exhibited a significant antimicrobial potential against all the tested microbes. Similarly, the Se NPs showed remarkable (89%) MB dye degradation potential in sunlight. Therefore, these green synthesized Se NPs may be used as an effective pharmacological agent and photocatalyst for the environmental remediation process in the future.

**Author Contributions:** D.I. and K.M. conceived and conducted the experimental work. D.I., A.A. and R.V. wrote the original manuscript draft; M.F.A. and A.F.A. validation and editing; A.K. validation and visualization; S.R.P. data analysis. R.S. and G.S.K. supervision, validation, and editing. All authors have read and agreed to the published version of the manuscript.

**Funding:** The authors sincerely thank the Researchers Supporting Project Number (RSP2023R436) King Saud University, Riyadh, Saudi Arabia.

**Institutional Review Board Statement:** Not applicable.

**Informed Consent Statement:** Not applicable.

**Data Availability Statement:** Not applicable.

**Conflicts of Interest:** There are no conflicts to declare.

## References

1. Sangeetha, J.; Thangadurai, D.; David, M.; Abdullah, M.A. Recent Advances in Applications of Nanomaterials for Water Remediation. In *Environmental Biotechnology*, 1st ed.; Apple Academic Press: New York, NY, USA, 2016; pp. 119–140.
2. Lim, E.-K.; Kim, T.; Paik, S.; Haam, S.; Huh, Y.-M.; Lee, K. Nanomaterials for theranostics: Recent advances and future challenges. *Chem. Rev.* **2015**, *115*, 327–394. [[CrossRef](#)]
3. Ihtisham, M.; Noori, A.; Yadav, S.; Sarraf, M.; Kumari, P.; Brestic, M.; Imran, M.; Jiang, F.; Yan, X.; Rastogi, A. Silver nanoparticle's toxicological effects and phytoremediation. *Nanomaterials* **2021**, *11*, 2164. [[CrossRef](#)] [[PubMed](#)]
4. Baig, N.; Kammakam, I.; Falath, W. Nanomaterials: A review of synthesis methods, properties, recent progress, and challenges. *Mater. Adv.* **2021**, *2*, 1821–1871. [[CrossRef](#)]
5. Majumdar, M.; Dubey, A.; Goswami, R.; Misra, T.K.; Roy, D.N. In vitro and in silico studies on the structural and biochemical insight of anti-biofilm activity of andrographanin from *Andrographis paniculata* against *Pseudomonas aeruginosa*. *World J. Microbiol. Biotechnol.* **2020**, *36*, 143. [[CrossRef](#)] [[PubMed](#)]
6. Tran, P.A.; O'Brien-Simpson, N.; Reynolds, E.C.; Pantarat, N.; Biswas, D.P.; O'Connor, A.J. Low cytotoxic trace element selenium nanoparticles and their differential antimicrobial properties against *S. aureus* and *E. coli*. *Nanotechnology* **2015**, *27*, 045101. [[CrossRef](#)] [[PubMed](#)]
7. Indhira, D.; Krishnamoorthy, M.; Ameen, F.; Bhat, S.A.; Arumugam, K.; Ramalingam, S.; Priyan, S.R.; Kumar, G.S. Biomimetic facile synthesis of zinc oxide and copper oxide nanoparticles from *Elaeagnus indica* for enhanced photocatalytic activity. *Environ. Res.* **2022**, *212*, 113323. [[CrossRef](#)]
8. Lu, F.; Astruc, D. Nanocatalysts and other nanomaterials for water remediation from organic pollutants. *Coord. Chem. Rev.* **2020**, *408*, 213180. [[CrossRef](#)]
9. Parmar, J.; Jang, S.; Soler, L.; Kim, D.-P.; Sánchez, S. Nano-photocatalysts in microfluidics, energy conversion and environmental applications. *Lab Chip* **2015**, *15*, 2352–2356. [[CrossRef](#)]
10. Gupta, A.; Mumtaz, S.; Li, C.-H.; Hussain, I.; Rotello, V.M. Combatting antibiotic-resistant bacteria using nanomaterials. *Chem. Soc. Rev.* **2019**, *48*, 415–427. [[CrossRef](#)]
11. Badawi, A.K.; Abd Elkodous, M.; Ali, G.A.M. Recent advances in dye and metal ion removal using efficient adsorbents and novel nano-based materials: An overview. *RSC Adv.* **2021**, *11*, 36528–36553. [[CrossRef](#)]
12. Sakr, T.M.; Korany, M.; Katti, K.V. Selenium nanomaterials in biomedicine—An overview of new opportunities in nanomedicine of selenium. *J. Drug Deliv. Sci. Technol.* **2018**, *46*, 223–233. [[CrossRef](#)]
13. Huang, Y.; Su, E.; Ren, J.; Qu, X. The recent biological applications of selenium-based nanomaterials. *Nano Today* **2021**, *38*, 101205. [[CrossRef](#)]
14. Patwardhan, S.V.; Staniland, S.S. Conventional methods to prepare nanomaterials. In *Green Nanomaterials: From Bioinspired Synthesis to Sustainable Manufacturing of Inorganic Nanomaterials*; IOP Publishing: Bristol, UK, 2019; pp. 4–21.
15. Ghoreishi, S.M.; Behpour, M.; Mortazavi, M.; Khoobi, A. Fabrication of a graphene oxide nano-sheet modified electrode for determination of dopamine in the presence of tyrosine: A multivariate optimization strategy. *J. Mol. Liq.* **2016**, *215*, 31–38. [[CrossRef](#)]
16. Mosleh, M.; Ghoreishi, S.M.; Masoum, S.; Khoobi, A. Determination of quercetin in the presence of tannic acid in soft drinks based on carbon nanotubes modified electrode using chemometric approaches. *Sens. Actuators B Chem.* **2018**, *272*, 605–611. [[CrossRef](#)]
17. Vollath, D. Nanomaterials an introduction to synthesis, properties and application. *Environ. Eng. Manag. J.* **2008**, *7*, 865–870.
18. Makarov, V.V.; Love, A.J.; Sinityna, O.V.; Makarova, S.S.; Yaminsky, I.V.; Taliansky, M.E.; Kalinina, N.O. “Green” nanotechnologies: Synthesis of metal nanoparticles using plants. *Acta Nat. (англоязычная версия)* **2014**, *6*, 35–44. [[CrossRef](#)]
19. Gebre, S.H.; Sendeku, M.G. New frontiers in the biosynthesis of metal oxide nanoparticles and their environmental applications: An overview. *SN Appl. Sci.* **2019**, *1*, 928. [[CrossRef](#)]
20. Bisht, N.; Phalswal, P.; Khanna, P.K. Selenium nanoparticles: A review on synthesis and biomedical applications. *Mater. Adv.* **2022**, *3*, 1415–1431. [[CrossRef](#)]
21. Roy, D.N.; Ahmad, I. Combating biofilm of ESKAPE pathogens from ancient plant-based therapy to modern nanotechnological combinations. In *A Complete Guidebook on Biofilm Study*; Elsevier: Amsterdam, The Netherlands, 2022; pp. 59–94.
22. Majumdar, M.; Khan, S.A.; Nandi, N.B.; Roy, S.; Panja, A.S.; Roy, D.N.; Misra, T.K. Green synthesis of iron nanoparticles for investigation of biofilm inhibition property. *ChemistrySelect* **2020**, *5*, 13575–13583. [[CrossRef](#)]
23. Manjunatha, C.; Preran Rao, P.; Bhardwaj, P.; Raju, H.; Ranganath, D. New insights into synthesis, morphological architectures and biomedical applications of elemental selenium nanostructures. *Biomed. Mater.* **2020**, *16*, 022010. [[CrossRef](#)]
24. Jiang, H.; Wang, R.; Zhou, F.; Wu, Y.; Li, S.; Huo, G.; Ye, J.; Hua, C.; Wang, Z. Preparation, physicochemical characterization, and cytotoxicity of selenium nanoparticles stabilized by *Oudemansiella raphanipies* polysaccharide. *Int. J. Biol. Macromol.* **2022**, *211*, 35–46. [[CrossRef](#)] [[PubMed](#)]

25. Ezhuthupurakkal, P.B.; Polaki, L.R.; Suyavaran, A.; Subastri, A.; Sujatha, V.; Thirunavukkarasu, C. Selenium nanoparticles synthesized in aqueous extract of *Allium sativum* perturbs the structural integrity of Calf thymus DNA through intercalation and groove binding. *Mater. Sci. Eng. C* **2017**, *74*, 597–608. [[CrossRef](#)] [[PubMed](#)]
26. Yilmaz, M.T.; Ispirli, H.; Taylan, O.; Dertli, E. A green nano-biosynthesis of selenium nanoparticles with Tarragon extract: Structural, thermal, and antimicrobial characterization. *LWT* **2021**, *141*, 110969. [[CrossRef](#)]
27. Fresneda, M.A.R.; Martín, J.D.; Bolívar, J.G.; Cantos, M.V.F.; Bosch-Estévez, G.; Moreno, M.F.M.; Merroun, M.L. Green synthesis and biotransformation of amorphous Se nanospheres to trigonal 1D Se nanostructures: Impact on Se mobility within the concept of radioactive waste disposal. *Environ. Sci. Nano* **2018**, *5*, 2103–2116. [[CrossRef](#)]
28. dos Santos Souza, L.M.; Dibo, M.; Sarmiento, J.J.P.; Seabra, A.B.; Medeiros, L.P.; Lourenço, I.M.; Kobayashi, R.K.T.; Nakazato, G. Biosynthesis of selenium nanoparticles using combinations of plant extracts and their antibacterial activity. *Curr. Res. Green Sustain. Chem.* **2022**, *5*, 100303. [[CrossRef](#)]
29. Majumdar, M.; Singh, V.; Misra, T.K.; Roy, D.N. In silico studies on structural inhibition of SARS-CoV-2 main protease Mpro by major secondary metabolites of *Andrographis paniculata* and *Cinchona officinalis*. *Biologia* **2022**, *77*, 1373–1389. [[CrossRef](#)] [[PubMed](#)]
30. Chandra, H.; Patel, D.; Kumari, P.; Jangwan, J.S.; Yadav, S. Phyto-mediated synthesis of zinc oxide nanoparticles of *Berberis aristata*: Characterization, antioxidant activity and antibacterial activity with special reference to urinary tract pathogens. *Mater. Sci. Eng. C* **2019**, *102*, 212–220. [[CrossRef](#)]
31. Srinivasan, R.; Aruna, A.; Lee, J.S.; Kim, M.; Shivakumar, M.S.; Natarajan, D. Antioxidant and antiproliferative potential of bioactive molecules ursolic acid and thujone isolated from *Memecylon edule* and *Elaeagnus indica* and their inhibitory effect on topoisomerase II by molecular docking approach. *BioMed Res. Int.* **2020**, *2020*, 8716927. [[CrossRef](#)]
32. RameshKannan, N.; Nayagam, A.A.J.; Gurunagara, S.; Muthukumar, B.; Ekambaram, N.; Manimaran, A. Photochemical screening from *Elaeagnus indica* activity against human pathogens and cancer cells. *Adv. Biol. Res.* **2013**, *7*, 95–103.
33. Srinivasan, R.; Aruna, A.; Manigandan, K.; Pugazhendhi, A.; Kim, M.; Shivakumar, M.S.; Natarajan, D. Phytochemical, antioxidant, antimicrobial and antiproliferative potential of *Elaeagnus indica*. *Biocatal. Agric. Biotechnol.* **2019**, *20*, 101265. [[CrossRef](#)]
34. Natarajan, R.K.; Nayagam, A.A.J.; Gurunagarajan, S.; Muthukumar, N.E.; Manimaran, A. *Elaeagnus indica* mediated green synthesis of silver nanoparticles and its potent toxicity against human pathogens. *World Appl. Sci. J.* **2013**, *23*, 1314–1321.
35. Alagesan, V.; Venugopal, S. Green synthesis of selenium nanoparticle using leaves extract of *withania somnifera* and its biological applications and photocatalytic activities. *Bionanoscience* **2019**, *9*, 105–116. [[CrossRef](#)]
36. Vijayakumar, T.P.; Benoy, M.D.; Duraimurugan, J.; Kumar, G.S.; Shkir, M.; Maadeswaran, P.; Kumar, A.S.; Kumar, K.A.R. Hydrothermal synthesis of CuO/g-C<sub>3</sub>N<sub>4</sub> nanosheets for visible-light driven photodegradation of methylene blue. *Diam. Relat. Mater.* **2022**, *121*, 108735. [[CrossRef](#)]
37. Abdel-Moneim, A.-M.E.; El-Saadony, M.T.; Shehata, A.M.; Saad, A.M.; Aldhumri, S.A.; Ouda, S.M.; Mesalam, N.M. Antioxidant and antimicrobial activities of *Spirulina platensis* extracts and biogenic selenium nanoparticles against selected pathogenic bacteria and fungi. *Saudi J. Biol. Sci.* **2022**, *29*, 1197–1209. [[CrossRef](#)]
38. Kokila, K.; Elavarasan, N.; Sujatha, V. *Diospyros montana* leaf extract-mediated synthesis of selenium nanoparticles and their biological applications. *New J. Chem.* **2017**, *41*, 7481–7490. [[CrossRef](#)]
39. Shahbaz, M.; Akram, A.; Raja, N.I.; Mukhtar, T.; Mehak, A.; Fatima, N.; Ajmal, M.; Ali, K.; Mustafa, N.; Abasi, F. Antifungal activity of green synthesized selenium nanoparticles and their effect on physiological, biochemical, and antioxidant defense system of mango under mango malformation disease. *PLoS ONE* **2023**, *18*, e0274679. [[CrossRef](#)]
40. Anu, K.; Singaravelu, G.; Murugan, K.; Benelli, G. Green-synthesis of selenium nanoparticles using garlic cloves (*Allium sativum*): Biophysical characterization and cytotoxicity on vero cells. *J. Clust. Sci.* **2017**, *28*, 551–563. [[CrossRef](#)]
41. Thanh, N.T.K.; Maclean, N.; Mahiddine, S. Mechanisms of nucleation and growth of nanoparticles in solution. *Chem. Rev.* **2014**, *114*, 7610–7630. [[CrossRef](#)]
42. Hosseinpour, L.; Baharara, J.; Bostanabad, S.Z.; Darroudi, M. Plant-based synthesis of selenium nanoparticles using *Cordia myxa* fruit extract and evaluation of their cytotoxicity effects. *Inorg. Chem. Commun.* **2022**, *145*, 110030. [[CrossRef](#)]
43. Alizadeh, S.R.; Abbastabar, M.; Nosratabadi, M.; Ebrahimzadeh, M.A. High antimicrobial, cytotoxicity, and catalytic activities of biosynthesized Selenium nanoparticles using *Crocus caspius* extract. *Arab. J. Chem.* **2023**, *16*, 104705. [[CrossRef](#)]
44. Nayak, V.; Singh, K.R.B.; Singh, A.K.; Singh, R.P. Potentialities of selenium nanoparticles in biomedical science. *New J. Chem.* **2021**, *45*, 2849–2878. [[CrossRef](#)]
45. Pandey, S.; Awasthee, N.; Shekher, A.; Rai, L.C.; Gupta, S.C.; Dubey, S.K. Biogenic synthesis and characterization of selenium nanoparticles and their applications with special reference to antibacterial, antioxidant, anticancer and photocatalytic activity. *Bioprocess Biosyst. Eng.* **2021**, *44*, 2679–2696. [[CrossRef](#)] [[PubMed](#)]
46. Nath, S.; Ghosh, S.K.; Panigahi, S.; Thundat, T.; Pal, T. Synthesis of selenium nanoparticle and its photocatalytic application for decolorization of methylene blue under UV irradiation. *Langmuir* **2004**, *20*, 7880–7883. [[CrossRef](#)]
47. Hassanien, R.; Abed-Elmageed, A.A.I.; Husein, D.Z. Eco-friendly approach to synthesize selenium nanoparticles: Photocatalytic degradation of sunset Yellow Azo Dye and anticancer activity. *ChemistrySelect* **2019**, *4*, 9018–9026. [[CrossRef](#)]
48. Menon, S.; Agarwal, H.; Shanmugam, V.K. Catalytic degradation of industrial dyes using biosynthesized selenium nanoparticles and evaluating its antimicrobial activities. *Sustain. Environ. Res.* **2021**, *31*, 2. [[CrossRef](#)]

49. Hosnedlova, B.; Kepinska, M.; Skalickova, S.; Fernandez, C.; Ruttkay-Nedecky, B.; Peng, Q.; Baron, M.; Melcova, M.; Opatrilova, R.; Zidkova, J. Nano-selenium and its nanomedicine applications: A critical review. *Int. J. Nanomed.* **2018**, *13*, 2107–2128. [[CrossRef](#)] [[PubMed](#)]
50. He, H.; Liu, C.; Shao, C.; Wu, Y.; Huang, Q. Green synthesis of ultrasmall selenium nanoparticles (SeNPs) using *Hericium erinaceus* polysaccharide (HEP) as nanozymes for efficient intracellular antioxidation. *Mater. Lett.* **2022**, *317*, 132079. [[CrossRef](#)]
51. Tinggi, U. Selenium: Its role as antioxidant in human health. *Environ. Health Prev. Med.* **2008**, *13*, 102–108. [[CrossRef](#)]

**Disclaimer/Publisher's Note:** The statements, opinions and data contained in all publications are solely those of the individual author(s) and contributor(s) and not of MDPI and/or the editor(s). MDPI and/or the editor(s) disclaim responsibility for any injury to people or property resulting from any ideas, methods, instructions or products referred to in the content.